# ORIGINAL RESEARCH

# Targeting Hypoxia-Inducible Factor-1α/Pyruvate Dehydrogenase Kinase 1 Axis by Dichloroacetate Suppresses Bleomycin-induced Pulmonary Fibrosis

Justin Goodwin[1], Hyunsung Choi[1], Meng-hsiung Hsieh[1], Michael L. Neugent[1], Jung-Mo Ahn[2], Heather N. Hayenga[3], Pankaj K. Singh[4], David B. Shackelford[5], In-Kyu Lee[6], Vladimir Shulaev[7], Shanta Dhar[8,9], Norihiko Takeda[10], and Jung-whan Kim[1]

[1]Department of Biological Sciences, [2]Department of Chemistry and Biochemistry, and [3]Department of Bioengineering, University of Texas at Dallas, Richardson, Texas; [4]Eppley Institute for Research in Cancer and Allied Diseases, University of Nebraska Medical Center, Omaha, Nebraska; [5]Department of Pulmonary and Critical Care Medicine, David Geffen School of Medicine, University of California, Los Angeles, California; [6]Section of Endocrinology, Department of Internal Medicine, Kyungpook National University Hospital, School of Medicine, Kyungpook National University, Daegu, Republic of Korea; [7]Department of Biological Sciences, College of Arts and Sciences, University of North Texas, Denton, Texas; [8]Department of Biochemistry and Molecular Biology and [9]Sylvester Comprehensive Cancer Center, Miller School of Medicine, University of Miami, Miami, Florida; and [10]Department of Cardiovascular Medicine, Graduate School of Medicine, University of Tokyo, Tokyo, Japan

## Abstract

Hypoxia has long been implicated in the pathogenesis of fibrotic diseases. Aberrantly activated myofibroblasts are the primary pathological driver of fibrotic progression, yet how various microenvironmental influences, such as hypoxia, contribute to their sustained activation and differentiation is poorly understood. As a defining feature of hypoxia is its impact on cellular metabolism, we sought to investigate how hypoxia-induced metabolic reprogramming affects myofibroblast differentiation and fibrotic progression, and to test the preclinical efficacy of targeting glycolytic metabolism for the treatment of pulmonary fibrosis. Bleomycin-induced pulmonary fibrotic progression was evaluated in two independent, fibroblast-specific, promoter-driven, hypoxia-inducible factor (*Hif*) *1A* knockout mouse models and in glycolytic inhibitor, dichloroacetate-treated mice. Genetic and pharmacological approaches were used to explicate the role of metabolic reprogramming in myofibroblast differentiation. Hypoxia significantly enhanced transforming growth factor-β–induced myofibroblast differentiation through HIF-1α, whereas overexpression of the critical HIF-1α–mediated glycolytic switch, pyruvate dehydrogenase kinase 1 (PDK1) was sufficient to activate glycolysis and potentiate myofibroblast differentiation, even in the absence of HIF-1α. Inhibition of the HIF-1α/PDK1 axis by genomic deletion of *Hif1A* or pharmacological inhibition of PDK1 significantly attenuated bleomycin-induced pulmonary fibrosis. Our findings suggest that HIF-1α/PDK1–mediated glycolytic reprogramming is a critical metabolic alteration that acts to promote myofibroblast differentiation and fibrotic progression, and demonstrate that targeting glycolytic metabolism may prove to be a potential therapeutic strategy for the treatment of pulmonary fibrosis.

**Keywords:** fibroblasts; hypoxia inducible factor-1α; pulmonary fibrosis; pyruvate dehydrogenase kinase1; dichloroacetate

## Clinical Relevance

Our study reveals a critical biological and clinical consideration for studying metabolic alterations in myofibroblast activation and fibrotic progression. This study further identifies a targetable key metabolic regulatory site for the treatment of pulmonary fibrosis. Perhaps most promising is the observation that dichloroacetate has been used safely and effectively on humans to treat metabolic disorders for over 40 years, which allows for potentially rapid clinical translation toward the treatment of pulmonary fibrosis.

Pulmonary fibrosis is a progressive and irreversible lung disease with a poor life expectancy of 2–5 years (1, 2). Among various cell types that contribute to fibrotic progression, aberrantly activated myofibroblasts serve as a major pathologic contributor to progressive pulmonary fibrosis (3–5). Myofibroblasts accumulate in fibrotic lesions and secrete excessive extracellular matrix proteins, such as collagen (Col) type 1, resulting in distortion of pulmonary structure and impairment of contractile capacity (6, 7). In addition, myofibroblasts have been shown to recruit inflammatory cells by secreting various cytokines, leading to aggravation of inflammation (3, 8). These pathological features of myofibroblasts collectively contribute to fibrotic initiation and progression. Despite numerous investigations seeking therapeutic options for the prevention and treatment of pulmonary fibrosis, no clinically targetable strategies that can directly inhibit myofibroblast fibrotic activation have been developed (9–12).

A hallmark feature of chronic tissue injury and fibrosis is the presence of hypoxia (13, 14). Mechanisms underlying hypoxia in tissue injury, like fibrosis, include inadequate blood supply due to vascular damage and infiltration of high-oxygen-consuming inflammatory cells. The microenvironmental nature of tissue hypoxia causes induction of the master transcription factor for oxygen homeostasis, hypoxia-inducible factor (HIF)-1. HIF-1 is composed of oxygen-sensitive HIF-1α and constitutively active HIF-1β subunits (15, 16). In the presence of sufficient oxygen, HIF-1α is hydroxylated by prolyl hydroxylases, with molecular oxygen as an essential cofactor. Hydroxylated HIF-1α is then recognized by von Hippel Lindau protein, targeting HIF-1α for proteasomal degradation (17–21). Stabilized HIF-1α, under hypoxic conditions, when heterodimerized with HIF-1β, transactivates target genes involved in cellular hypoxic adaptation, such as metabolic reprogramming into anaerobic glycolysis (22).

HIF-1α has been shown to play critical roles in fibrotic progression of various organs, including the lungs (23–26). Studies by our group and others using cell type–specific knockout or overexpression of hypoxic signaling pathways suggest that diverse cell types differentially respond to hypoxia, and further exhibit unique hypoxic phenotypes (27–35). This suggests that the functional contributions of HIF-1α signaling to pulmonary fibrosis are context and cell type specific via multiple mechanistic pathways. Yet, how the hypoxic microenvironment or HIF-1α signaling specifically affects the biology of fibroblasts, the major cell population that is activated, accumulates, and differentiates into extracellular matrix (ECM)–producing myofibroblasts during the development of pulmonary fibrosis, has not been elucidated.

During tissue injury and inflammation, the accumulation of hypoxic areas results in HIF-1–mediated anaerobic glycolysis, which provides essential metabolic reprogramming for the survival of hypoxic cells. We (36) and Papandreou and colleagues (37) previously demonstrated that pyruvate dehydrogenase kinase (PDK)-1 is a direct HIF-1 target gene, and that PDK-1 induction is a key metabolic switch for cellular hypoxic adaptation by augmenting glycolysis and suppressing mitochondrial respiration. This metabolic switch allows hypoxic cells to not only optimize oxygen consumption rate, but to suppress the toxic burst of mitochondrial reactive oxygen species. HIF-1α/PDK-1 axis has been well characterized as crucial to metabolic reprogramming for survival and tumor growth in various human cancers (38, 39). Moreover, recent studies have demonstrated that HIF-1α/PDK1–mediated metabolic reprogramming is essentially linked to differentiation of hematopoietic and embryonic stem cells, macrophages, and T cells, arguing for the importance of PDK1-mediated glycolytic metabolism in cellular metabolic homeostasis across various cell types (40–43).

Recently, glycolytic metabolism has been shown to play an important role in pulmonary fibrotic progression (44). Inhibition of the key glycolytic enzyme, phosphofructokinase, was effective in attenuating pulmonary fibrosis progression in the isolated primary lung fibroblasts from patients with idiopathic pulmonary fibrosis (IPF) and pulmonary fibrosis animal models (44). Accordingly, highly elevated lactic acid levels, indicative of up-regulated glycolysis, have been observed in patients with IPF, and is associated with augmented myofibroblast differentiation (45, 46). These results suggest that glycolytic reprograming is an important contributor to myofibroblast activation and differentiation, thereby promoting pulmonary fibrosis progression.

In this study, we sought to determine if fibroblast HIF-1α signaling essentially contributes to myofibroblast differentiation and profibrotic progression via PDK1-mediated glycolytic reprogramming. We demonstrate that fibroblast-specific ablation of *Hif1A* attenuates the number of α-smooth muscle actin (α-SMA)–expressing myofibroblasts, as well as collagen accumulation in bleomycin-induced murine pulmonary fibrosis. In addition, dichloroacetate (DCA), a potent PDK inhibitor (47, 48), effectively inhibits transforming growth factor (TGF)-β–mediated myofibroblast differentiation *in vitro* as well as bleomycin-induced lung fibrosis *in vivo*. These previously undescribed metabolic alterations in fibroblasts may prove to be exploitable as a novel therapeutic strategy for pulmonary fibrosis treatment.

## Methods

### Mice and Bleomycin-induced Pulmonary Fibrosis Model

Wild-type Friend leukemia virus, strain B mice were purchased from Jackson Laboratory. To generate fibroblast-specific *Hif1A* knockout mice, mice carrying locus of X-over P1 recombinase recognition sites in the *Hif1A* gene (*Hif1A^{fl/fl}*) were bred to mice expressing Cre recombinase (Cre) driven by the fibroblast-specific protein (FSP) 1 promoter (*FSP1-Cre*) (30, 49, 50),

or bred to mice expressing tamoxifen-dependent Cre recombinase (CreER[T2]) driven by the Col1α1 promoter (*Col1α1-CreER*) (51, 52). All mice were backcrossed to a more than 15th-generation congenic Friend leukemia virus, strain B background. For CreER induction, tamoxifen was administered via intraperitoneal injection (100 mg/kg; Sigma) every 24 hours for 5 consecutive days, 6 days before bleomycin inhalation. To generate bleomycin-induced pulmonary fibrosis, 6- to 8-week-old mice inhaled 0.05 U bleomycin sulfate intratracheally (Sigma) (53). DCA was orally administered via drinking water containing 1.5 g/L sodium DCA (Sigma) on the same day as bleomycin inhalation. All mice were maintained in the pathogen-free Animal Resource Center at University of Texas at Dallas (Richardson, TX). All experimental procedures using mice were approved by the University of Texas at Dallas Institutional Animal Care and Use Committees.

### Cell Culture and Hypoxia

Human normal lung fibroblasts, CCD19Lu (ATCC CCL210; American Type Culture Collection) and mouse normal lung fibroblasts, Mlg 2,908 (American Type Culture Collection CCL206) were used in this study. Primary lung fibroblasts derived from patients with IPF (PCR-70-0213 and PCR-70-0214) were purchased from Asterand Bioscience. Cells were maintained in minimum essential medium Eagle or high-glucose (4,500 mg/ml) Dulbecco's modified Eagle's medium (DMEM) supplemented with 10% FBS and 1% penicillin/streptomycin. For mouse primary lung fibroblast culture, mice were perfused with PBS containing 2 mM EDTA, and excised lung tissues were incubated in DMEM with 2 mg/ml of collagenase for 2 hours at 37°C. Red blood cells were removed using $1\times$ RBC lysis buffer (eBioscience). Primary lung fibroblasts were resuspended with DMEM containing 10% FBS and 1% penicillin/streptomycin. Cells were maintained at 37°C in a humidified atmosphere of 5% $CO_2$/95% air. For hypoxia experiments, cells were maintained with 1% $O_2$, 5% $CO_2$, and 94% $N_2$ gas in humidified hypoxic workstation (INVIVO$_2$ 300; Ruskinn Technology).

### Transfection and Stable Cell Line Establishment

Small interfering RNA (siRNA) targeting HIF-1α or PDK1 (ONTARGETplus SMARTpool; Dharmacon) was transfected with a pool of four specific siRNAs complexed using lipofectamine 3,000 (Invitrogen). For lentivirus-mediated stable knockdown or overexpression, pLKO.1-based small hairpin (sh) HIF-1α I (Mission TRC shRNA, TRCN0000003810; Sigma), II (Mission TRC shRNA, TRCN0000010819; Sigma), and pLenti-GIII-CMV-GFP-PDK1 (LV259395; ABM Inc.) was transfected into 293T cells with viral packaging plasmids, psPAX2 and pMD2.G, using lipofectamine 3,000 (Invitrogen). Cells were incubated with viral supernatant containing 8 μg/ml polybrene. Transduced cells were selected with 1 μg/ml of puromycin.

### Statistical Analysis

Statistical analysis was performed using StatPlus, Version v5 (AnalystSoft Inc.), Microsoft Excel, and GraphPad Prism 6.0 (GraphPad Software Inc.). Differences between conditions were examined using two-tailed Student's *t* test, or one-way ANOVA with multiple comparison *post hoc* test. All data are expressed as means (±SE).

All other experiments were performed as described in the METHODS in the data supplement.

## Results

### Fibroblast-Specific *Hif1A* Deletion Attenuates Bleomycin-induced Pulmonary Fibrosis

Hypoxia has been implicated in tissue injuries and fibrosis (14, 25). We verified tissue hypoxia in fibrotic lungs, as indicated by the formation of pimonidazole adducts, which specifically define severely hypoxic cells (<1% $O_2$), as well as immunohistochemical detection of HIF-1α (*see* Figure E1A in the data supplement). Pulmonary fibrosis is characterized by cellular heterogeneity in which various cell types collectively contribute to the pathogenesis of the disease (3). Immunohistochemical analysis revealed that HIF-1α was induced in α-SMA–expressing myofibroblasts in fibrotic lesions (Figure 1A). This shows that fibroblasts, the major cell population that is differentiated into ECM-producing myofibroblasts during fibrotic progression, are exposed to hypoxic microenvironments and express HIF-1α. To determine the role of fibroblast HIF-1α in pulmonary fibrosis, we created a murine model for targeted deletion of the *Hif1A* gene by crossing mice with *Hif1A$^{fl/fl}$* alleles, in which exon 2 is flanked with locus of X-over P1 sites (54), with mice possessing a *cre* allele driven by the promoter of FSP1 (55). FSP1 may be expressed in various subpopulations of mesenchymal cells (56, 57). However, cells isolated from the lungs of *FSP1-Cre; Rosa26-LSL-tdTomato* mice displayed robust expression of fibroblast-specific markers, with minimal expression of other mesenchymal markers (Figure E1B). This indicates that the resulting progeny (*FSP1-Cre; Hif1A$^{fl/fl}$*) possess a highly specific fibroblast *Hif1A* deletion (49, 50, 55). Quantitative RT-PCR analysis showed that FSP1-driven Cre recombinase achieved an *Hif1A* exon 2 deletion efficiency of 73% (Figure E1C). Mice harboring the fibroblast *Hif1A* deletion have normal viability postnatally and do not display any obvious phenotypes when housed under standard sterile barrier conditions. Upon intratracheal bleomycin inhalation, wild-type mice (*Hif1A$^{fl/fl}$*) developed significant levels of pulmonary tissue damage with the accumulation of α-SMA$^+$ myofibroblasts as well as elevated collagen deposition (Figure 1B). In contrast, fibroblast *Hif1A* knockout (*FSP1-Cre; Hif1A$^{fl/fl}$*) mice displayed significant reduction of α-SMA$^+$ myofibroblasts and collagen accumulation in fibrotic lesions. Expression of α-SMA is a classical marker for differentiating fibroblasts; however, its expression is not confined to myofibroblasts, but can be expressed in various other cell types, including blood vessel–associated pericytes (58, 59). To ensure that we restricted our analysis to fibroblast-specific α-SMA expression, we performed double-immunofluorescent staining for α-SMA and endothelial cell marker, CD34, which allowed us to exclude α-SMA and CD34 double-positive areas, indicative of pericyte-associated α-SMA expression. After excluding α-SMA$^+$ pericytes, we found that fibroblast *Hif1A* knockout mice showed significant reduction in α-SMA$^+$ myofibroblasts (Figure 1C). Hydroxyproline analysis of lung tissue showed significantly less collagen content in fibroblast *Hif1A* knockout mice compared with wild-type mice (Figure 1D). Next, we looked at markers of fibrotic progression in immunoblots of lung tissue from wild-type and fibroblast *Hif1A*
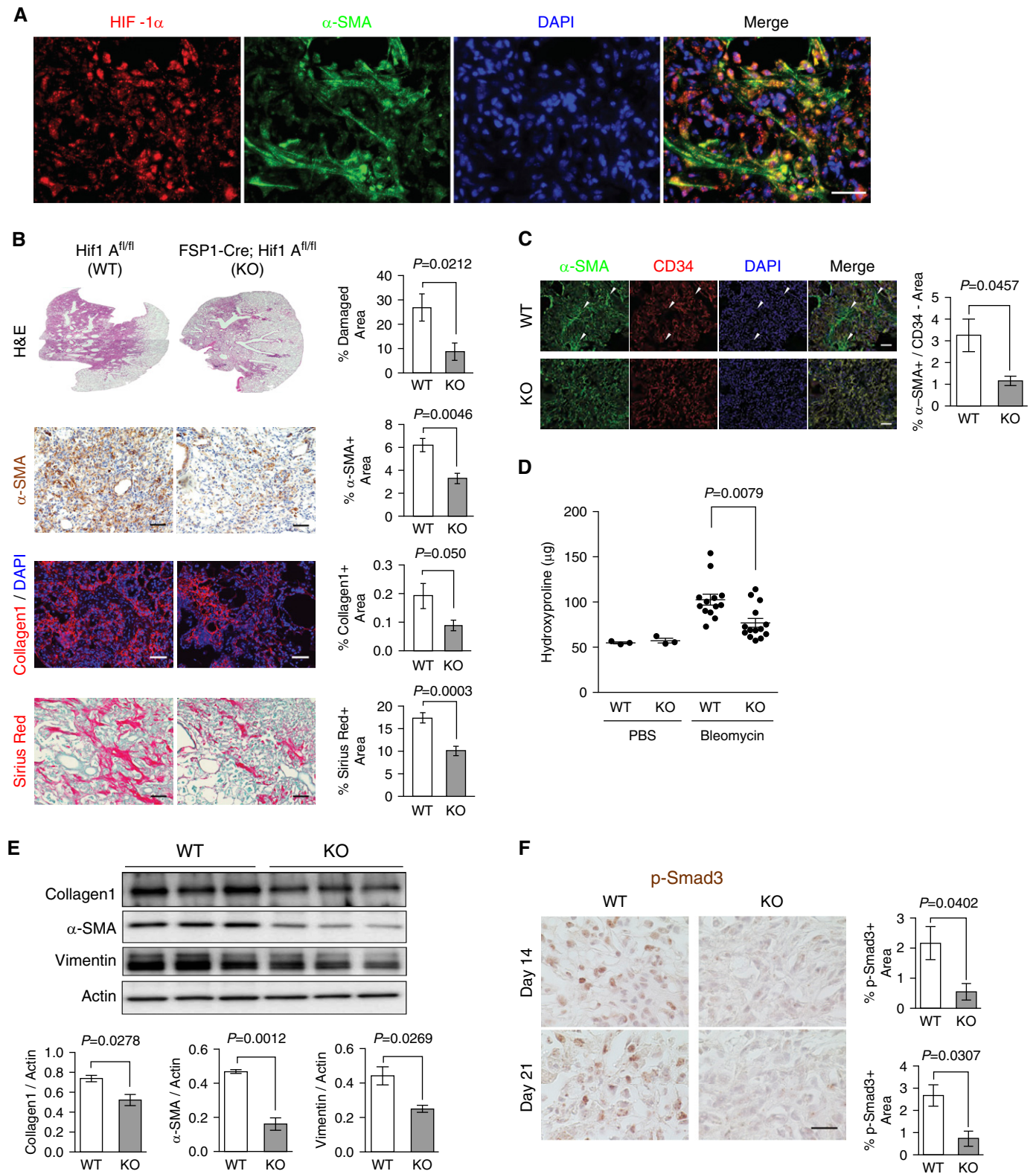
**Figure 1.** Fibroblast-specific protein (FSP) 1–driven fibroblast hypoxia-inducible factor (*Hif*) *1A* ablation attenuates pulmonary fibrosis. (*A*) Representative immunofluorescent images of colocalized HIF-1α (red) and α-smooth muscle actin (α-SMA; green) in bleomycin-induced fibrotic lung tissues. (*B*) Representative images and quantification of wild-type (WT; *Hif1A*^fl/fl^) and FSP1-driven, Cre recombinase (Cre)-mediated, fibroblast-specific *Hif1A* knockout (KO; *FSP1-Cre*; *Hif1A*^fl/fl^) composite hematoxylin and eosin (H&E) montage images of whole lung lobes, α-SMA immunohistochemistry (IHC), immunofluorescent collagen, and
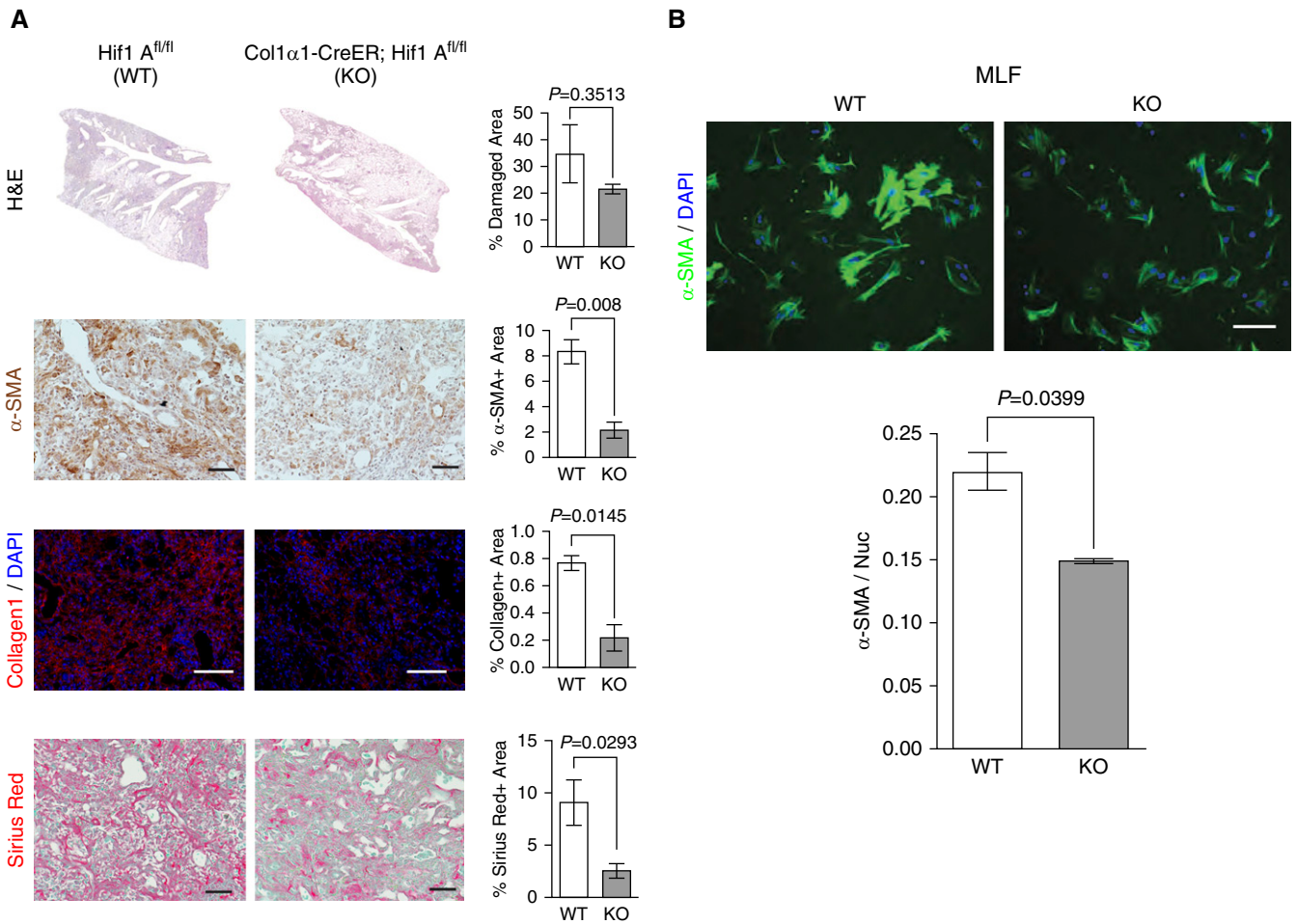
**Figure 2.** Col1α1-CreER–driven fibroblast *Hif1A* ablation attenuates pulmonary fibrosis. (*A*) Representative images and quantification of WT (*Hif1A^{fl/fl}*) and Col1α1-CreER–driven, fibroblast-specific *Hif1A* KO (*Col1α1-CreER*; *Hif1A^{fl/fl}*) composite H&E montage images of whole lung lobes, α-SMA IHC, immunofluorescent Col1, and Sirius red staining (*n* = 3–4 per group, 8–12 images per mouse were captured for quantification). (*B*) Representative immunocytochemistry and quantification of α-SMA in primary mouse lung fibroblasts isolated from WT and fibroblast *Hif1A* KO mice (*n* = 3 per group, 6–8 images per mouse were captured for quantification). Scale bars: 100 μm. Error bars represent the mean (±SEM). Two-tailed *t* test. MLF = mouse lung fibroblasts.

knockout mice, and found that consistent with histological and hydroxyproline analysis, lung tissue of HIF-1α–deficient fibroblasts contained less Col1, α-SMA, and vimentin (Figure 1E). As canonical TGF-β signaling through Smad3 is crucial for myofibroblast differentiation and fibrotic progression (55, 56), we looked at phosphorylated (p)-Smad3 at two different time points after bleomycin inhalation as an indicator of active fibrogenesis.

Fibroblast *Hif1A* knockout was associated with significantly reduced TGF-β signaling through Smad3 when compared with wild-type mouse lungs at 14 and 21 days after bleomycin inhalation (Figure 1F). This suggests that fibroblast *Hif1A* deletion suppresses myofibroblast differentiation throughout the fibrogenic phase in bleomycin-inhaled mice.

Pulmonary fibroblasts exhibit substantial heterogeneity, with subpopulations defined by distinct regional, morphological, and functional properties (3, 9, 60, 61). Implications for these heterogeneous populations of fibroblasts include variable contributions to disease progression and treatment response. To expand our investigation of the role of fibroblast HIF-1α in pulmonary fibrosis, we created an additional conditional fibroblast-specific *Hif1A* knockout using tamoxifen-inducible CreER(T2), the expression of

**Figure 1.** (Continued). Sirius red staining (*n* = 6–8 per group, 10–15 images per mouse were captured for quantification). (*C*) Representative images of α-SMA (green) and CD34 (red) double-immunofluorescent staining and quantification of α-SMA⁺/CD34⁻ areas in WT (*n* = 5) and fibroblast-specific *Hif1A* KO mice (*n* = 3, 8–10 images per mouse were captured for quantification). Arrowheads indicate α-SMA⁺/CD34⁻ areas. (*D*) Lung hydroxyproline content of WT and fibroblast *Hif1A* KO mice treated with PBS or bleomycin (*n* = 3 per PBS-treated group, *n* = 14 per bleomycin-treated group). (*E*) Western blot analysis and quantification of lung collagen (Col) 1, α-SMA, and vimentin expression in WT and fibroblast *Hif1A* KO mice treated with bleomycin (*n* = 3 per group). (*F*) Representative images and quantification of phosphorylated (p)-Smad3 IHC in WT and fibroblast *Hif1A* KO mice 14 days (*n* = 4 per group) and 21 days (*n* = 3 per group) after bleomycin treatment. Scale bar: 25 μm. All other scale bars: 100 μm. Error bars represent the mean (±SEM). Two-tailed *t* test.
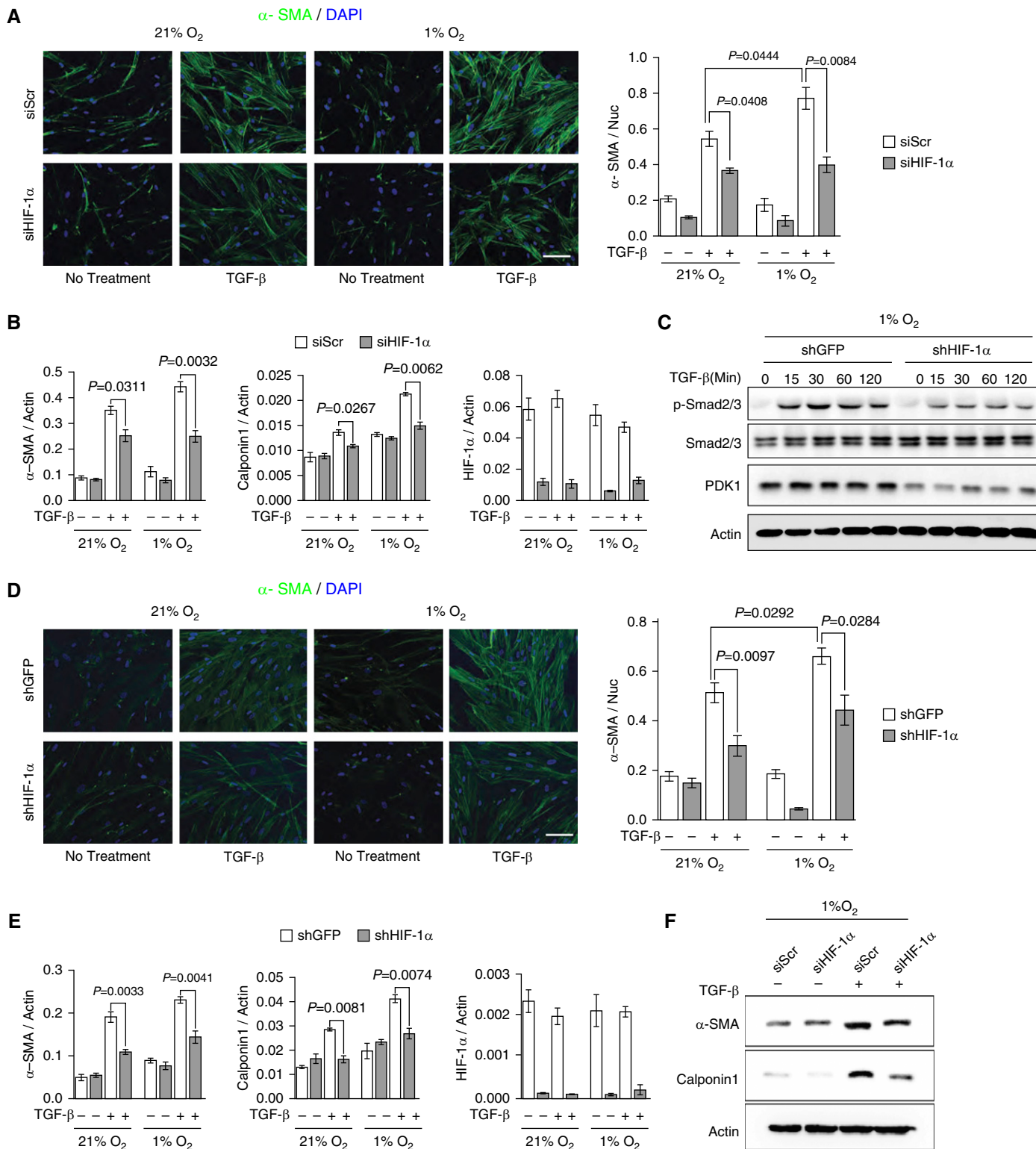
**Figure 3.** HIF-1α knockdown inhibits transforming growth factor (TGF)-β–induced myofibroblast differentiation. (*A*) Representative immunocytochemistry and quantification of α-SMA in small interfering (si) Scramble (Scr) and siHIF-1α fibroblasts derived from patients with idiopathic pulmonary fibrosis cultured in 21 and 1% $O_2$ and treated with 2 ng/ml TGF-β for 72 hours (*n* = 8 from four biologically independent experiments, five to six images were captured per group and normalized to nuclei for quantification). (*B*) Quantitative RT-PCR (qRT-PCR) analysis of α-SMA, calponin1, and HIF-1α mRNA expression in siScr and siHIF-1α idiopathic pulmonary fibroblasts (IPFs) cultured in 21 and 1% $O_2$ and treated with 2 ng/ml TGF-β for 72 hours (*n* = 6 from three biologically independent experiments). (*C*) Western blot analysis of p-Smad2/3, total Smad2/3, and pyruvate dehydrogenase kinase (PDK) 1 expression in small hairpin

which is driven by the Col1α1 promoter (*Col1α1-CreER*) (51, 52). Consistent with FSP1-specific *Hif1A* deletion, Col-Cre–mediated *Hif1A* knockout mice (*Col1α1-CreER; Hif1A$^{fl/fl}$*) exhibited significant attenuation of bleomycin-induced fibrotic progression indicated by less α-SMA$^+$ myofibroblasts and less collagen accumulation in the lungs (Figure 2A). Next, using an inducible fluorescent promoter, we sorted tdTomato$^+$ primary mouse lung fibroblasts from wild-type (*Col1α1-CreER; Rosa26-LSL-tdTomato*) and fibroblast *Hif1A* knockout (*Col1α1-CreER; Rosa26-LSL-tdTomato; Hif1A$^{fl/fl}$*) mice after bleomycin inhalation and looked at α-SMA expression (Figure 2B). We found that HIF-1α–deficient fibroblasts expressed significantly less α-SMA than wild-type fibroblasts, consistent with the reduction in α-SMA$^+$ myofibroblasts observed in histopathological analysis. Collectively, these results suggest that fibroblast-specific HIF-1α signaling is a critical component of pulmonary fibrosis.

## Hypoxia Promotes Myofibroblast Differentiation in an HIF-1α–Dependent Manner

Enhanced myofibroblast differentiation is the key phenotypic feature associated with pathological fibrotic progression. Therefore, we sought to determine whether hypoxia or HIF-1α accumulation enhances myofibroblast differentiation. Hypoxia alone (1% $O_2$) did not significantly increase α-SMA mRNA expression in primary fibroblasts derived from patients with IPF, despite induction of canonical HIF-1α target genes, hexokinase 2, phosphofructokinase1, 6-phosphofructo-2-kinase/fructose-2,6-biphosphatase 3, and PDK1 (Figure E2A). TGF-β is the primary profibrogenic cytokine responsible for inducing myofibroblast differentiation in IPF. Therefore, we sought to determine if hypoxia and HIF-1α augment TGF-β–induced myofibroblast differentiation. Hypoxia significantly enhanced

TGF-β–induced α-SMA and another myofibroblast marker, calponin1, compared with TGF-β induction in normoxia (21% $O_2$; Figures 3A and 3B). To determine if HIF-1α accounts for hypoxia-augmented myofibroblast differentiation, we genetically targeted HIF-1α expression in idiopathic pulmonary fibroblasts by siRNA. HIF-1α knockdown significantly reduced TGF-β–induced α-SMA and calponin expression in normoxic and hypoxic conditions (Figures 3A and 3B). Likewise, hypoxic induction of hexokinase 2 and PDK1 was effectively suppressed by siRNA-mediated knockdown of HIF-1α under hypoxic conditions (Figures E2A and E2B). Notably, phosphorylation of Smad2/3 was decreased in HIF-1α–deficient fibroblasts under hypoxic conditions (Figure 3C). As with our pathohistological analysis of p-Smad3 in fibroblast HIF-1α–deficient lung tissue, this further indicates that the loss of HIF-1α expression is associated with attenuated myofibroblast differentiation. Consistently, hypoxia enhanced TGF-β–induced α-SMA expression in normal human lung fibroblasts (HLFs), while shRNA-mediated stable knockdown of HIF-1α suppressed α-SMA and calponin expression (Figures 3D–3F and Figure E2C). These results indicate that hypoxia potentiates TGF-β–induced myofibroblast differentiation through HIF-1α signaling.

## PDK1 Promotes Myofibroblast Differentiation

Metabolic reprogramming has been shown to be crucial for myofibroblast differentiation and a profibrotic phenotype (44, 62). The critical contribution of fibroblast HIF-1α signaling to pulmonary fibrosis (Figures 1B and 2A) suggests that HIF-1α–mediated glycolytic reprogramming may be an important pathobiological step in fibrotic progression. Consistent with a previous study showing accumulation of lactate in patients with IPF (45, 46), bleomycin-induced fibrotic lungs have significantly higher levels of lactate, which is indicative of augmented glycolysis (Figure 4A). Furthermore, TGF-β

treatment resulted in increased intracellular and extracellular lactate accumulation in primary fibroblasts derived from patients with IPF (Figure 4B, Figure E3A). This lactate accumulation was abrogated after HIF-1α knockdown (Figure 4B), suggesting that HIF-1α is significantly responsible for increased glycolytic metabolism in TGF-β–induced myofibroblast differentiation. PDK1 is an essential metabolic switch induced by HIF-1α that directs pyruvate toward conversion into lactate, providing hypoxic cells with critical metabolic adaptations (36, 37). Analysis of microarray gene profile data from 137 control subjects and 255 patients with interstitial lung disease obtained from the Lung Genomics Research Consortium database (63–65) revealed that, along with α-SMA, PDK1 expression was significantly elevated in patients with interstitial lung disease (Figure 4C, Figure E3B). We suspected that the loss of PDK1 might considerably suppress myofibroblast differentiation by inhibiting HIF-1α–mediated glycolytic reprogramming. siRNA-mediated PDK1 knockdown effectively abolished pyruvate dehydrogenase (PDH) phosphorylation to a similar level as the PDK1 inhibitor, DCA, and significantly suppressed lactate accumulation in TGF-β–treated HLFs, indicating that PDK1 knockdown inhibits TGF-β–induced metabolic reprogramming (Figures 4D and 4E, Figure E3C). Importantly, we found that PDK1 knockdown resulted in significant decreases in TGF-β–mediated induction of myofibroblast markers, α-SMA and calponin1 (Figures 4F and 4G), suggesting that PDK1 is necessary for myofibroblast differentiation. Next, we sought to determine if forced overexpression of PDK1 renders fibroblasts prone to differentiation. Lentivirus (lenti)-PDK1–transduced fibroblasts have significantly higher PDK1 expression and lactate accumulation compared with control lenti-GFP fibroblasts (Figures E3D and E3E). Immunofluorescent staining demonstrated that PDK1-overexpressing fibroblasts

**Figure 3.** (Continued). (sh) GFP and shHIF-1α human lung fibroblasts (HLFs) cultured in 1% $O_2$ and treated with 5 ng/ml TGF-β (0–120 min). These results were observed in three independent experiments. (*D*) Representative immunocytochemistry and quantification of α-SMA in shGFP and shHIF-1α HLFs cultured in 21 and 1% $O_2$ and treated with 2 ng/ml TGF-β for 72 hours (*n* = 8 from four biologically independent experiments, five to six images were captured per group and normalized to nuclei for quantification). (*E*) qRT-PCR analysis of α-SMA, calponin1, and HIF-1α mRNA expression in shGFP and shHIF-1α HLFs cultured in 21 and 1% $O_2$ and treated with 2 ng/ml TGF-β for 72 hours (*n* = 6 from three biologically independent experiments). (*F*) Western blot analysis of α-SMA and calponin1 expression in siScr and siHIF-1α HLFs cultured in 1% $O_2$ and treated with 2 ng/ml TGF-β for 72 hours. These results were observed in three independent experiments. Scale bars: 100 μm. Error bars represent the mean (±SEM). One-way ANOVA with multiple comparison, *post hoc*.
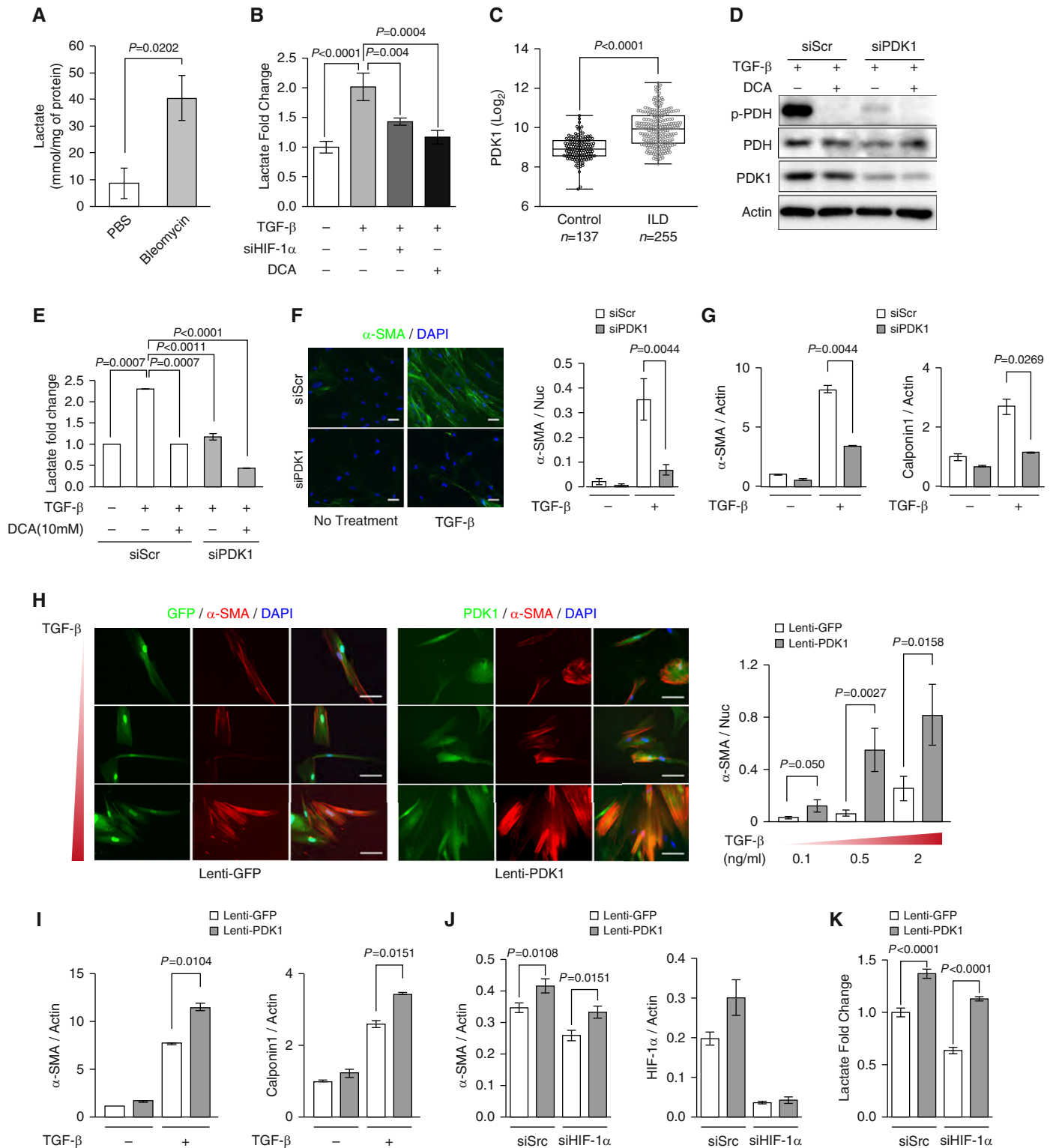
**Figure 4.** PDK1 promotes myofibroblast differentiation. (*A*) Lactate concentration of lung tissue from PBS- and bleomycin-treated mice (*n* = 4 per group). Two-tailed *t* test. (*B*) Extracellular lactate measurement in siScr or siHIF-1α IPFs treated with TGF-β or TGF-β + dichloroacetate (DCA; *n* = 6 from three biologically independent experiments). IPFs were treated with 2 ng/ml TGF-β and 10 mM DCA for 72 hours. (*C*) Microarray gene profile analysis of PDK1 expression between control subjects (*n* = 137) and patients with interstitial lung disease (ILD; *n* = 255), derived from the Lung Genomics Research Consortium database. Mann-Whitney *U* test. (*D*) Western blot analysis of p-pyruvate dehydrogenase (PDH), total PDH, and PDK1 expression in siScr and siPDK1 HLFs treated with 5 ng/ml TGF-β and 10 mM DCA for 24 hours. These results were

exhibited augmented myofibroblast differentiation characterized by enhanced α-SMA expression and morphological features of differentiation, as well as elevated levels of α-SMA and calponin1 mRNA (Figures 4H and 4I). Accordingly, PDK1 overexpression significantly increased lactate accumulation and PDH phosphorylation, even under DCA treatment (Figures E3F and E3G). This indicates that augmented glycolytic reprogramming through ectopic PDK1 overexpression potentiates TGF-β–induced myofibroblast differentiation.

HIF-1α was shown to have a putative binding site in the α-SMA promoter region (44), allowing for direct transcriptional regulation of α-SMA expression, independent of PDK1 induction or subsequent metabolic reprogramming. To determine the relative contributions of HIF-1α or PDK1 to myofibroblast differentiation, we performed siRNA-mediated HIF-1α knockdown in lenti-GFP and lenti-PDK1 fibroblasts, and measured expression of myofibroblast markers upon TGF-β activation. PDK1 overexpression increased α-SMA expression in HIF-1α–deficient fibroblasts (Figure 4J). Furthermore, PDK1 overexpression was able to augment glycolysis in the absence of HIF-1α (Figure 4K), suggesting that a significant contribution of the profibrotic effects of HIF-1α derive from glycolytic reprogramming through PDK1, and further suggesting that inhibition of this metabolic switch underlies the antifibrotic mechanism of action of DCA.

### Targeting PDKs by DCA Suppresses Myofibroblast Differentiation

Despite considerable effort, therapeutic strategies targeting fibroblast activation and differentiation remain inadequate. The potent role of PDK1 in modulating myofibroblast differentiation through metabolic reprogramming prompted us to approach pharmacological PDK1 inhibition. We employed DCA, a potent PDK inhibitor that rewires cellular glycolytic metabolism to mitochondrial oxidative phosphorylation. DCA treatment abrogated TGF-β–induced lactate production in idiopathic pulmonary fibroblasts and HLFs (Figures 4B and 5A). Metabolic flux analysis showed that DCA treatment suppressed extracellular acidification rate and increased oxygen consumption rate, indicative of increased pyruvate flux through the citric acid cycle (Figure 5B). These results indicate that DCA treatment effectively suppresses PDK-mediated glycolytic reprogramming in pulmonary fibroblasts. Importantly, PDK inhibition by DCA treatment significantly attenuated α-SMA expression in TGF-β–treated idiopathic pulmonary fibroblasts in a dose-dependent manner (Figures 5C and 5D). Expression of another myofibroblast marker, calponin1, was also reduced by DCA treatment in idiopathic pulmonary fibroblasts (Figure 5D). Furthermore, DCA treatment resulted in decreased Smad-dependent (p-Smad2/3) and Smad-independent (p-extracellular signal-regulated kinase [ERK] 1/2) TGF-β signaling, indicative of reduced myofibroblast differentiation (Figure 5E). Consistently, DCA treatment suppressed α-SMA protein and mRNA expression in both HLFs and normal mouse lung fibroblasts (Figures 5F and 5G, Figures E4A and E4B). PDK inhibition by DCA can exert cytotoxicity through mitochondrial respiratory reactive oxygen species burst (36, 66), raising a possibility that decreased expression of myofibroblast markers of DCA treatment may result from global inhibition of protein synthesis or mRNA transcription. However, DCA treatment did not affect mRNA or protein stability in transcriptional inhibitor, actinomycin D, or protein synthesis inhibitor, cycloheximide, -treated fibroblasts, respectively (Figures E4C–E4E), indicating that DCA specifically suppresses myofibroblastic activation. These results suggest that the HIF-1α/PDK1 axis is crucial for myofibroblast differentiation and can be exploited for *in vivo* antifibrotic therapeutic strategies.

### DCA Suppresses Bleomycin-induced Pulmonary Fibrosis

The antifibrotic effects of genetic and pharmacological inhibition of the HIF-1α/PDK1 axis provide a rationale for accessing PDK inhibition as a potential therapeutic strategy for pulmonary fibrosis. To determine the preclinical efficacy of PDK inhibition in pulmonary fibrotic progression, we administered DCA in bleomycin-inhaled mice and examined the fibrotic progression. Because DCA has a high oral availability, we added DCA into sterile drinking water (0.75–1.5 g/L). With this concentration, our calculation shows that the amount of DCA administered to each mouse was roughly 50–100 mg/kg/d, which has been shown to exert potent therapeutic effects without apparent toxic side effects in recent studies (48, 67). In accordance with lactate accumulation in bleomycin-induced fibrotic lungs (Figure 4A), we observed phosphorylation of PDH in fibrotic regions, indicative of PDK activity and higher levels of glycolysis (Figure 6A). With our administration regimen, phosphorylation of PDH was dramatically reduced by DCA. Consistent with fibroblast HIF-1α deficiency (Figures 1B and 2A),

Figure 4. (Continued). observed from three independent experiments. (E) Extracellular lactate measurement in siScr or siPDK1 HLFs treated with TGF-β or TGF-β + DCA (n = 6 from three biologically independent experiments). IPFs were treated with 2 ng/ml TGF-β and 10 mM DCA for 48 hours. (F) Representative immunocytochemistry and quantification of α-SMA in siScr and siPDK1 HLFs treated with 2 ng/ml TGF-β for 72 hours (n = 6 from three biologically independent experiments, 5–10 images were captured per group and normalized to nuclei for quantification). Two-tailed t test. (G) qRT-PCR analysis of α-SMA and calponin1 mRNA expression in siScr and siPDK1 HLFs treated with 2 ng/ml TGF-β for 72 hours (n = 4 from two biologically independent experiments). Two-tailed t test. (H) Representative immunocytochemistry and quantification of α-SMA in lentivirus (lenti)-GFP and lenti-PDK1 HLFs treated with the indicated TGF-β concentrations for 72 hours (n = 6 from three biologically independent experiments, 5–10 images were captured per group and normalized to nuclei for quantification). (I) qRT-PCR analysis of α-SMA and calponin1 mRNA expression in lenti-GFP and lenti-PDK1 HLFs treated with 2 ng/ml TGF-β for 72 hours (n = 4 from two biologically independent experiments). Two-tailed t test. (J) qRT-PCR analysis of α-SMA and HIF-1α expression in siScr/lenti-GFP or lenti-PDK1, and siHIF-1α/lenti-GFP or lenti-PDK1 HLFs treated with 2 ng/ml TGF-β for 72 hours (n = 8 from four biologically independent experiments). (K) Extracellular lactate measurement in siScr/lenti-GFP or lenti-PDK1, and siHIF-1α/lenti-GFP or lenti-PDK1 HLFs treated with 2 ng/ml TGF-β for 72 hours (n = 8 from four biologically independent experiments). Scale bars: 100 μm. Error bars represent the mean (±SEM). One-way ANOVA with multiple comparison, *post hoc*, unless otherwise noted.
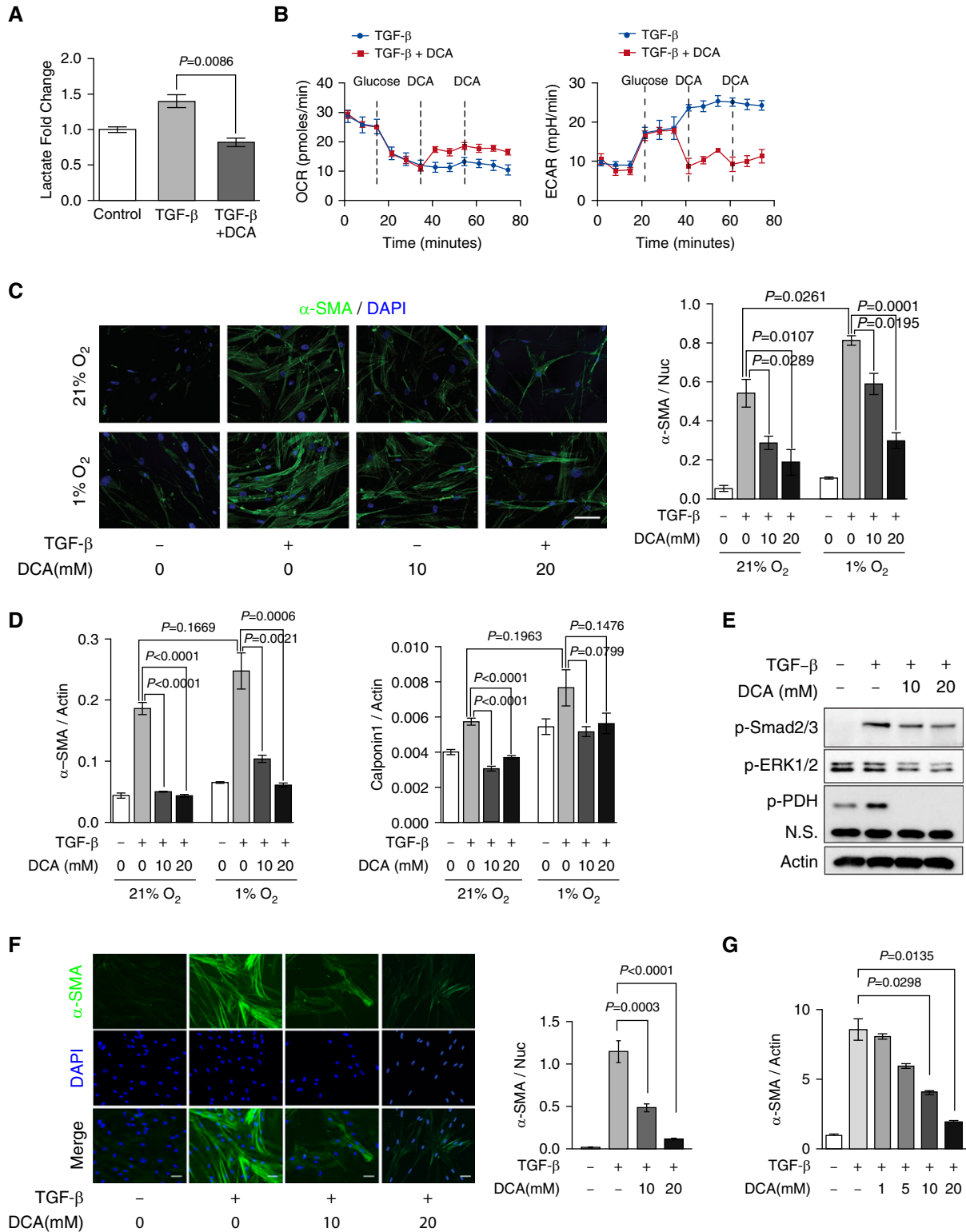
**Figure 5.** DCA inhibits TGF-β–induced myofibroblast differentiation. (*A*) Extracellular lactate measurement in siScr or siHIF-1α HLFs treated with TGF-β or TGF-β + DCA (*n* = 6 from three biologically independent experiments). HLFs were treated with 5 ng/ml TGF-β and 10 mM DCA for 48 hours. (*B*) Metabolic flux analysis of oxygen consumption rate (OCR) and extracellular acidification rate (ECAR) in IPFs treated with 2 ng/ml TGF-β for 48 hours (*n* = 6 from two biologically independent experiments). IPFs were glucose starved for 2 hours before the assay and then treated sequentially with 10 mM glucose, 10 mM DCA, and 20 mM DCA. (*C*) Representative immunocytochemistry and quantification of α-SMA in control and DCA-treated IPFs cultured in 21 and 1% O₂ and treated with 2 ng/ml TGF-β and 10 or 20 mM DCA for 72 hours (*n* = 8 from four biologically independent experiments, five to six images were captured

histopathological evaluation revealed that DCA treatment significantly attenuated bleomycin-induced fibrosis, which is characterized by a reduction of $\alpha$-SMA$^+$ myofibroblasts and collagen deposition (Figures 6B and 6C). Notably, we did not witness any phenotypic differences in the early stages of fibrotic progression (10 d after bleomycin inhalation; Figure E5A). This suggests that the antifibrotic effects of DCA are not derived from suppression of acute lung responses during the inflammatory phase of bleomycin inhalation. We further characterized the fibrotic burden between vehicle- and DCA-treated mice by analyzing the hydroxyproline content of the lungs. Consistent with histopathological evaluation, DCA-treated mice exhibited significantly lower hydroxyproline content (Figure 6D). This was associated with decreased protein and mRNA expression of myofibroblast markers, including Col1, $\alpha$-SMA, and vimentin (Figures 6E and 6F). Likewise, TGF-$\beta$ signaling through Smad3 was significantly reduced in DCA-treated mice, recapitulating the effects of fibroblast *Hif1A* knockout in inhibiting myofibroblast differentiation and fibrotic progression (Figure 6G). In addition to analyzing expression of myofibroblasts and extracellular matrix content, BAL fluid from DCA-treated mice had reduced expression of fibrosis-related cytokines, TNF-$\alpha$, IL-1$\beta$, and CCL2, compared with vehicle-treated mice (Figure 6H). These preclinical studies suggest that inhibition of PDK by DCA attenuates bleomycin-induced pulmonary fibrosis.

## Discussion

Hypoxia is a predominant microenvironmental component of fibrotic tissues that influences various cell types within fibrotic areas through inadequate oxygen availability (27–34), yet the cell type–specific expression and functional contributions of hypoxic signaling to the development of pulmonary fibrosis remain largely unknown. Our study modulating the hypoxic response within fibroblasts derived from bleomycin-induced pulmonary fibrosis animal models, as well as patients with IPF, reveals that hypoxia and the hypoxia-inducible transcription factor, HIF-1, augments myofibroblast differentiation and fibrotic progression. Our study further demonstrates that glycolytic reprogramming essentially enhances the profibrotic activation of pulmonary fibroblasts. We identified HIF-1$\alpha$/PDK1–mediated glycolytic reprogramming as a critical regulatory step necessary for myofibroblast differentiation in pulmonary fibrosis. Genetic or pharmacological inhibition of the HIF-1$\alpha$/PDK1 axis significantly attenuated bleomycin-induced pulmonary fibrotic progression (Figures 1B, 2A, and B6B), providing proof of principle for targeting glycolytic metabolism in the treatment of pulmonary fibrosis. In line with our findings, recent studies suggested that glycolytic metabolism is an integral component of myofibroblast differentiation in pulmonary fibrosis. Xie and colleagues (44) further demonstrated that targeting glycolytic flux via inhibition of a rate-limiting glycolytic enzyme, 6-phosphofructo-2-kinase, effectively reduced myofibroblast differentiation and fibrotic progression. Together, these findings provide a compelling rationale to target glycolytic metabolism as a potential therapeutic strategy for pulmonary fibrosis.

HIF-1$\alpha$ signaling has been implicated in the development of fibrotic diseases of various organs, including lung, kidney, liver, and adipose tissues (25, 35, 68, 69). However, the fibroblast-specific activation and functional contribution of HIF-1$\alpha$ signaling to fibrogenic progression has not been fully elucidated. Our study using two independent FSP1- and Col1$\alpha$1-driven *Hif1A* knockout mice found that loss of fibroblast-specific HIF-1$\alpha$ signaling significantly suppressed bleomycin-induced pulmonary fibrosis. These findings must be tempered with the consideration that neither FSP1 nor Col1$\alpha$1 are truly specific for fibroblasts, and are known to be expressed in other mesenchymal cell types, such as macrophages and osteoblasts, and may even be expressed temporally or spatially in other as-yet-unidentified cell populations (51, 57). As of now, no single fibroblast-specific marker that fully excludes other various cell types has been identified, and this is made more challenging by the substantial heterogeneity that exists even among pulmonary fibroblasts (60, 61). Therefore, although we cannot exclude the possibility that *Hif1A* deletion in these additional cell types contributes to the antifibrotic phenotypes observed in our *in vivo* models, the use of two independent and highly fibroblast-specific, promoter-driven *Hif1A* knockout mice provides strong, compelling evidence that intrinsic fibroblast HIF-1$\alpha$ signaling plays a critical role in myofibroblast differentiation and fibrotic progression.

Given the multifaceted nature of HIF-1$\alpha$ signaling, it is not surprising that HIF-1$\alpha$ acts on promoting profibrotic machinery through multiple mechanisms. Previous studies have shown that HIF-1$\alpha$ transcriptionally induces $\alpha$-SMA expression in fibroblasts, implicating HIF-1$\alpha$ in the direct regulation of myofibroblast differentiation (44). Notably, PDK1 overexpression potentiated myofibroblast differentiation in the absence of HIF-1$\alpha$ signaling (Figure 4J), suggesting a significant contribution of the profibrogenic effects are derived from PDK1-augmented glycolysis, in addition to direct HIF-1$\alpha$ regulation of $\alpha$-SMA. HIF-1$\alpha$ signaling is reciprocally linked with various inflammatory pathways (70). In particular, various inflammatory mediators have been identified as HIF-1$\alpha$ targets (71). This raises the possibility that fibroblast *Hif1A* deletion might have exerted antifibrotic effects through suppression of inflammatory cell recruitment into fibrotic

**Figure 5.** (Continued). per group and normalized to nuclei for quantification). (*D*) qRT-PCR analysis of $\alpha$-SMA and calponin1 mRNA expression in control and DCA-treated IPFs cultured in 21 and 1% $O_2$ and treated with 2 ng/ml TGF-$\beta$ and 10 or 20 mM DCA for 72 hours (*n* = 6 from three biologically independent experiments). (*E*) Western blot analysis of p-Smad2/3, p-extracellular signal-regulated kinase (ERK) 1/2, and p-PDH expression in control and DCA-treated HLFs treated with 2 ng/ml TGF-$\beta$ with or without 10 mM DCA for 1 hour. These results were observed in three independent experiments. N.S. = nonspecific band. (*F*) Representative immunocytochemistry and quantification of $\alpha$-SMA in control and DCA-treated HLFs cultured in 1% $O_2$ and treated with 2 ng/ml TGF-$\beta$ and 10 or 20 mM DCA for 72 hours (*n* = 6 from three biologically independent experiments, five images were captured per group and normalized to nuclei for quantification). (*G*) qRT-PCR analysis of $\alpha$-SMA mRNA expression in control and DCA-treated IPFs cultured in 1% $O_2$ and treated with 2 ng/ml TGF-$\beta$ and 1–20 mM DCA for 72 hours (*n* = 6 from three biologically independent experiments). Scale bars: 100 $\mu$m. Error bars represent the mean ($\pm$SEM). One-way ANOVA with multiple comparison, *post hoc*.
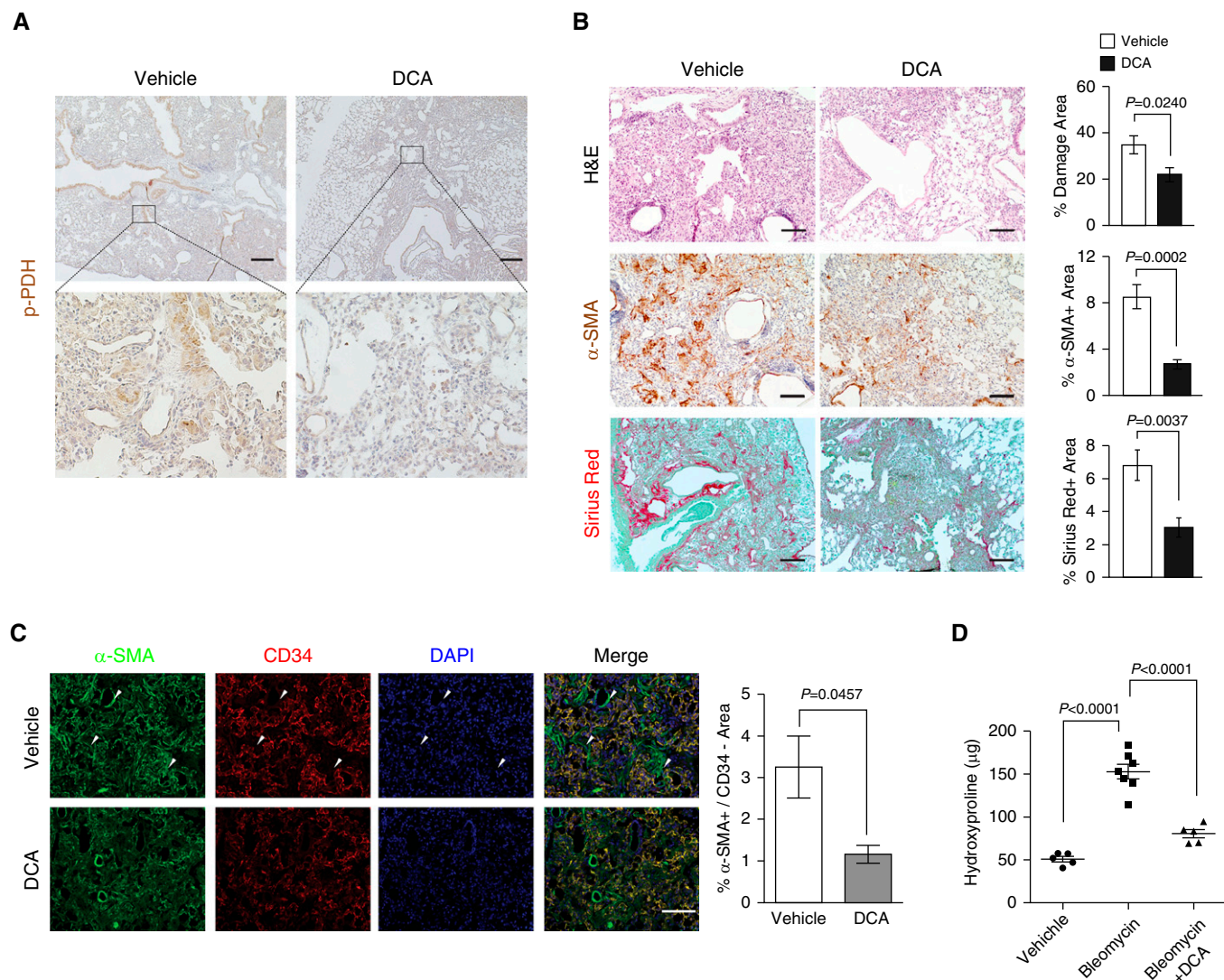
**Figure 6.** DCA suppresses bleomycin-induced pulmonary fibrosis. (*A*) Representative IHC images of p-PDH in bleomycin-induced pulmonary fibrotic mice treated with vehicle or DCA. Scale bars, 500 μm (inset, 100 μm). (*B*) Representative images and quantification of H&E, α-SMA IHC, and Sirius red staining in bleomycin-administered mice treated *ad libitum* with vehicle (*n* = 7) or 1.5 g/L DCA containing water (*n* = 8, 8–10 images per mouse were captured for quantification). Two-tailed *t* test. (*C*) Representative images of α-SMA (green) and CD34 (red) double-immunofluorescent staining and quantification of α-SMA⁺/CD34⁻ areas in vehicle- and DCA-treated mice (*n* = 3–5, 8–10 images per mouse were captured for quantification). Arrowheads indicate α-SMA⁺/CD34⁻ areas. Two-tailed *t* test. (*D*) Lung hydroxyproline content of PBS-treated or bleomycin-induced pulmonary fibrotic mice treated *ad libitum* with vehicle or 1.5 g/L DCA containing water (*n* = 5 PBS-treated group, *n* = 7 bleomycin-treated group, *n* = 5 DCA-treated group). (*E*) Western blot analysis and quantification of lung Col1, α-SMA, and vimentin expression in PBS-treated or bleomycin-induced pulmonary fibrotic mice treated *ad libitum* with vehicle or 1.5 g/L DCA containing water (*n* = 3 per group). (*F*) qRT-PCR analysis of Col1, α-SMA, and calponin1 mRNA expression in PBS-treated or bleomycin-induced pulmonary fibrotic mice treated *ad libitum* with vehicle or 1.5 g/L DCA containing water (*n* = 6 per group). (*G*) Representative images and quantification of p-Smad3 IHC in bleomycin-induced pulmonary fibrotic mice treated *ad libitum* with vehicle or 1.5 g/L DCA containing water (*n* = 3 per group). Scale bar: 25 μm. Two-tailed *t* test. (*H*) qRT-PCR analysis of TNF-α, IL-1β, and CCL2 mRNA expression from BAL of PBS-treated or bleomycin-induced pulmonary fibrotic mice treated *ad libitum* with water containing vehicle or 1.5 g/L DCA for 14 days (*n* = 3 per group). Scale bars: 100 μm unless otherwise noted. Error bars represent the mean (±SEM). One-way ANOVA with multiple comparison, *post hoc*, unless otherwise noted.

tissues; however, histopathological evaluation of inflammatory cells, including macrophages, T cells, B cells, and mast cells, revealed no differences between bleomycin-treated wild-type and fibroblast *Hif1A* knockout fibrotic lungs (Figure E6).

HIF-1α has been shown to be regulated by various signaling pathways, including the TGF-β pathway. McMahon and colleagues (72) reported that TGF-β1 enhances HIF-1α protein stability. Consistent with this study, we observed that

TGF-β treatment increases the level of HIF-1α protein in normal and fibrotic tissue–derived fibroblasts (Figure E7). Along with TGF-β–mediated HIF-1α activation, our findings of the crucial role of HIF-1α in sustaining TGF-β signaling

**E**

Vehicle | Bleomycin | Bleomycin+DCA

Collagen1
α–SMA
Vimentin
Actin

Collagen1 / Actin — P=0.0004, P=0.036
α–SMA / Actin — P=0.023, P=0.050
Vimentin / Actin — P=0.007, P=0.0013

**F**

Collagen1 / Actin — P=0.0004, P=0.0180
α–SMA / Actin — P=0.0003, P=0.0063
Calponin1 / Actin — P=0.0008, P=0.018

**G**

Vehicle | DCA

p-Smad3

% p-Smad3+ Area — P=0.0472

**H**

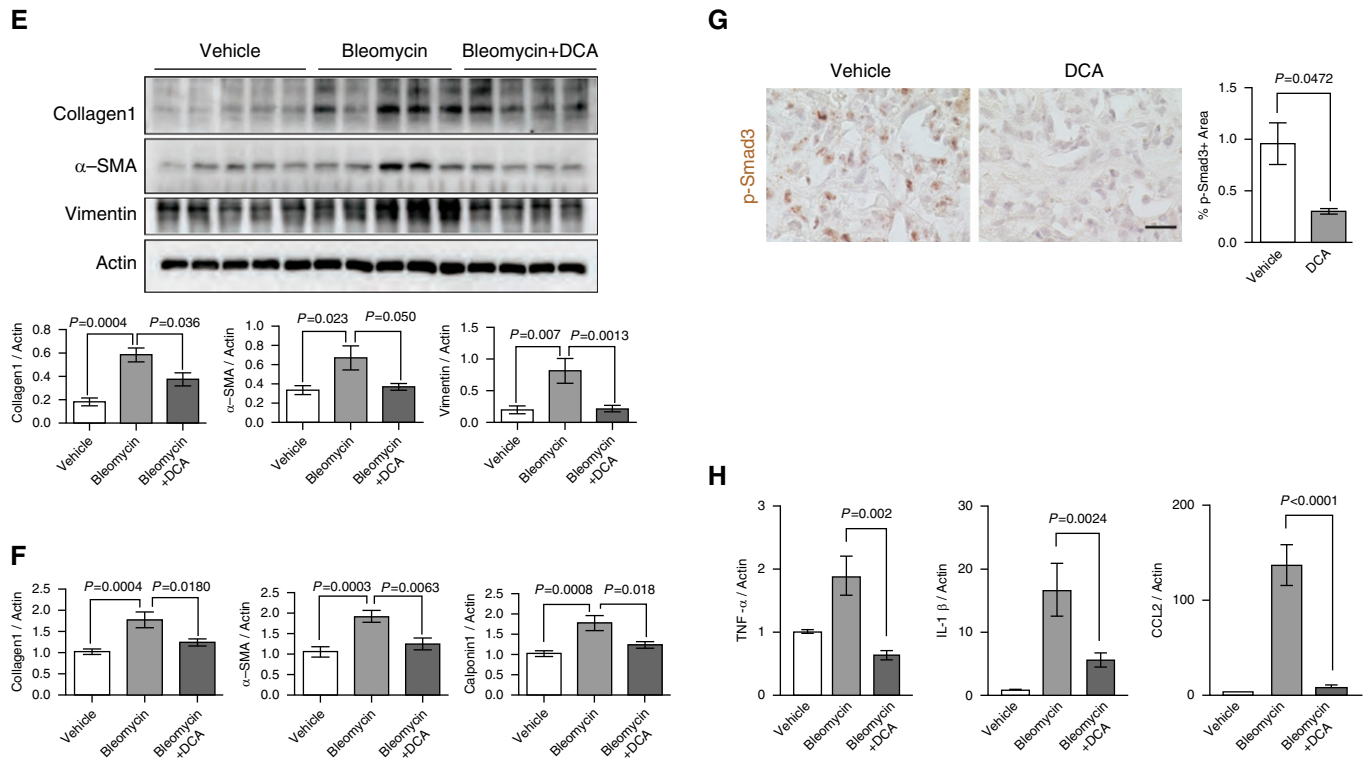TNF-α / Actin — P=0.002
IL-1 β / Actin — P=0.0024
CCL2 / Actin — P<0.0001

**Figure 6.** (Continued).

(Figure 3C) suggest a convergence of TGF-β signaling and hypoxia in the activation of HIF-1α, proposing a potential positive-feedback loop of HIF-1α/TGF-β in the progression of pulmonary fibrosis. Although the molecular mechanisms underpinning this functional interaction between HIF-1α and TGF-β signaling remains to be elucidated, our study provides evidence that PDK1-mediated glycolytic reprogramming may be a key regulatory node in this feedback loop, and, more importantly, PDK inhibition by DCA may sever this vicious fibrotic loop to exert antifibrotic effects.

Since its first report in the late 1960s, DCA has been studied as a potential therapeutic agent to treat congenital mitochondrial diseases, lactic acidosis, and their associated complications (47, 48, 73). In light of recent advancements in understanding cancer metabolism, in which glycolytic reprogramming provides cellular bioenergetics, as well as anabolic precursors for cancer cell survival and proliferation, a number of studies have reported that DCA may have promising anticancer effects via perturbing glycolytic phenotypes and mitochondrial functions (74–76). In

addition, DCA has been evaluated for other pathological conditions, including diabetic cardiomyopathy, restenosis, pulmonary hypertension, and heart failure (77–80). These studies highlight the potential clinical feasibility of targeting PDK-mediated glycolytic metabolism via DCA for the treatment of various human diseases, including fibrotic diseases. Given that the pulmonary fibrotic process is highly heterogeneous and regulated by multiple cell types, an inherent limitation in which systemic administration of DCA will not selectively target fibroblasts, may affect the interpretation of our data. However, our findings of significantly reduced fibrosis in fibroblast-specific Hif1A knockout systems argue that DCA exerts its antifibrotic effects at least partially by targeting HIF-1α/PDK1 axis in fibroblasts. Nonetheless, it should be acknowledged that other key cellular components, such as pulmonary alveolar epithelial cells and inflammatory cells, may be metabolically affected by systemic DCA treatment, which, in turn, could contribute to antifibrotic activities. Intriguingly, our recent study has demonstrated that the HIF-1α/PDK1 axis plays a critical role in migratory capabilities of macrophages, and

that DCA treatment dramatically suppresses macrophage mobilization into necrotic or tumor tissues (81). This raises a possibility that DCA treatment may affect recruitment of bone marrow–derived progenitor cells, such as fibrocytes, the mesenchymal progenitor cell population that has been implicated in pulmonary fibrosis. Moreover, a recent study by Eckle and colleagues (82) showed that alveolar-specific deletion of Hif1A aggravates lung inflammation in acute lung injury models. This illuminates the heterogeneous complexity of hypoxic and metabolic alterations of key cellular components in pulmonary fibrotic progression.

Although the precise molecular mechanism by which glycolytic metabolism affects myofibrogenic and fibrotic processes is yet to be defined, studies in cancer cells have revealed how cellular metabolic alterations can significantly impact the epigenetic state of a cell (83). These epigenetic modifications may explain the sustained activation of myofibroblasts, even in the absence of fibrogenic cues (84–87). Another potential mechanism underlying myofibroblast differentiation by the

HIF-1α/PDK1 axis may be elevated lactate in the fibrotic microenvironment, which may provide a more permissive bioenergetics cue for fibroblasts, accelerating lactate oxidation into pyruvate, which may be further metabolized and used for the citric acid cycle and mitochondrial respiration, as previously described in the brain and tumor microenvironment (88–91). Alternatively, lactate accumulation may create an acidic microenvironment, which may facilitate proteolytic activation of latent TGF-β, promoting myofibroblast differentiation and fibrotic progression (92). Further preclinical as well as clinical studies will be crucial for an integrated understanding of the cellular and molecular link between accelerated myofibroblast differentiation and cell type–specific glycolytic metabolism during pulmonary fibrotic disease progression.

This study is, to our knowledge, the first to identify fibroblast HIF-1α/PDK1 axis as a targetable key metabolic regulatory site for the treatment of pulmonary fibrosis. This previously undescribed metabolic regulatory site in the pathogenesis of pulmonary fibrosis may prove to be a novel therapeutic target with the potential for rapid clinical translation, as DCA has been used successfully and safely on humans with rare metabolic disorders for more than 40 years (47, 67). More importantly, virtually all major organs and tissues are susceptible to the development of irreversible and fatal fibrosis. If the involvement of fibroblast glycolytic reprogramming is not limited to pulmonary fibrosis, but clinically relevant to other types of fibrosis, this further underscores the need for a better understanding of metabolic alterations associated with the abnormal wound healing process and organ fibrosis. ■

## References

1. American Thoracic Society: idiopathic pulmonary fibrosis: diagnosis and treatment. International consensus statement. American Thoracic Society (ATS), and the European Respiratory Society (ERS). *Am J Respir Crit Care Med* 2000;161:646–664.
2. American Thoracic Society; European Respiratory Society. American Thoracic Society/European Respiratory Society international multidisciplinary consensus classification of the idiopathic interstitial pneumonias. This joint statement of the American Thoracic Society (ATS), and the European Respiratory Society (ERS) was adopted by the ATS board of directors, June 2001 and by the ERS Executive Committee, June 2001. *Am J Respir Crit Care Med* 2002;165:277–304.
3. Wynn TA. Integrating mechanisms of pulmonary fibrosis. *J Exp Med* 2011;208:1339–1350.
4. Barkauskas CE, Noble PW. Cellular mechanisms of tissue fibrosis. 7. New insights into the cellular mechanisms of pulmonary fibrosis. *Am J Physiol Cell Physiol* 2014;306:C987–C996.
5. Todd NW, Luzina IG, Atamas SP. Molecular and cellular mechanisms of pulmonary fibrosis. *Fibrogenesis Tissue Repair* 2012;5:11.
6. Kis K, Liu X, Hagood JS. Myofibroblast differentiation and survival in fibrotic disease. *Expert Rev Mol Med* 2011;13:e27.
7. Phan SH. The myofibroblast in pulmonary fibrosis. *Chest* 2002; 122(6 suppl):286S–289S.
8. Wilson MS, Wynn TA. Pulmonary fibrosis: pathogenesis, etiology and regulation. *Mucosal Immunol* 2009;2:103–121.
9. Noble PW, Barkauskas CE, Jiang D. Pulmonary fibrosis: patterns and perpetrators. *J Clin Invest* 2012;122:2756–2762.
10. Canestaro WJ, Forrester SH, Raghu G, Ho L, Devine BE. Drug treatment of idiopathic pulmonary fibrosis: systematic review and network meta-analysis. *Chest* 2016;149:756–766.
11. Loomis-King H, Flaherty KR, Moore BB. Pathogenesis, current treatments and future directions for idiopathic pulmonary fibrosis. *Curr Opin Pharmacol* 2013;13:377–385.
12. Spagnolo P, Wells AU, Collard HR. Pharmacological treatment of idiopathic pulmonary fibrosis: an update. *Drug Discov Today* 2015; 20:514–524.
13. Higgins DF, Kimura K, Iwano M, Haase VH. Hypoxia-inducible factor signaling in the development of tissue fibrosis. *Cell Cycle* 2008;7: 1128–1132.
14. Lokmic Z, Musyoka J, Hewitson TD, Darby IA. Hypoxia and hypoxia signaling in tissue repair and fibrosis. *Int Rev Cell Mol Biol* 2012;296: 139–185.
15. Wang GL, Semenza GL. Purification and characterization of hypoxia-inducible factor 1. *J Biol Chem* 1995;270:1230–1237.
16. Wang GL, Jiang BH, Rue EA, Semenza GL. Hypoxia-inducible factor 1 is a basic-helix-loop-helix-PAS heterodimer regulated by cellular $O_2$ tension. *Proc Natl Acad Sci USA* 1995;92:5510–5514.
17. Ivan M, Kondo K, Yang H, Kim W, Valiando J, Ohh M, et al. HIFα targeted for VHL-mediated destruction by proline hydroxylation: implications for $O_2$ sensing. *Science* 2001;292:464–468.
18. Jaakkola P, Mole DR, Tian YM, Wilson MI, Gielbert J, Gaskell SJ, et al. Targeting of HIF-α to the von Hippel-Lindau ubiquitylation complex by $O_2$-regulated prolyl hydroxylation. *Science* 2001; 292:468–472.
19. Yu F, White SB, Zhao Q, Lee FS. HIF-1α binding to VHL is regulated by stimulus-sensitive proline hydroxylation. *Proc Natl Acad Sci USA* 2001;98:9630–9635.
20. Maxwell PH, Wiesener MS, Chang GW, Clifford SC, Vaux EC, Cockman ME, et al. The tumour suppressor protein VHL targets hypoxia-inducible factors for oxygen-dependent proteolysis. *Nature* 1999;399:271–275.
21. Ohh M, Park CW, Ivan M, Hoffman MA, Kim TY, Huang LE, et al. Ubiquitination of hypoxia-inducible factor requires direct binding to the β-domain of the von Hippel-Lindau protein. *Nat Cell Biol* 2000;2: 423–427.
22. Semenza GL. Regulation of metabolism by hypoxia-inducible factor 1. *Cold Spring Harb Symp Quant Biol* 2011;76:347–353.
23. Higgins DF, Kimura K, Bernhardt WM, Shrimanker N, Akai Y, Hohenstein B, et al. Hypoxia promotes fibrogenesis *in vivo* via HIF-1 stimulation of epithelial-to-mesenchymal transition. *J Clin Invest* 2007;117:3810–3820.
24. Kimura K, Iwano M, Higgins DF, Yamaguchi Y, Nakatani K, Harada K, et al. Stable expression of HIF-1α in tubular epithelial cells promotes interstitial fibrosis. *Am J Physiol Renal Physiol* 2008;295: F1023–F1029.
25. Tzouvelekis A, Harokopos V, Paparountas T, Oikonomou N, Chatziioannou A, Vilaras G, et al. Comparative expression profiling in pulmonary fibrosis suggests a role of hypoxia-inducible factor-1α in disease pathogenesis. *Am J Respir Crit Care Med* 2007;176: 1108–1119.
26. Ueno M, Maeno T, Nomura M, Aoyagi-Ikeda K, Matsui H, Hara K, et al. Hypoxia-inducible factor-1α mediates TGF-β–induced PAI-1 production in alveolar macrophages in pulmonary fibrosis. *Am J Physiol Lung Cell Mol Physiol* 2011;300:L740–L752.
27. Blouw B, Song H, Tihan T, Bosze J, Ferrara N, Gerber HP, et al. The hypoxic response of tumors is dependent on their microenvironment. *Cancer Cell* 2003;4:133–146.
28. Cramer T, Yamanishi Y, Clausen BE, Förster I, Pawlinski R, Mackman N, et al. HIF-1α is essential for myeloid cell-mediated inflammation. *Cell* 2003;112:645–657.

29. Doedens AL, Stockmann C, Rubinstein MP, Liao D, Zhang N, DeNardo DG, et al. Macrophage expression of hypoxia-inducible factor-1 α suppresses T-cell function and promotes tumor progression. Cancer Res 2010;70:7465–7475.

30. Kim JW, Evans C, Weidemann A, Takeda N, Lee YS, Stockmann C, et al. Loss of fibroblast HIF-1α accelerates tumorigenesis. Cancer Res 2012;72:3187–3195.

31. Peyssonnaux C, Datta V, Cramer T, Doedens A, Theodorakis EA, Gallo RL, et al. HIF-1α expression regulates the bactericidal capacity of phagocytes. J Clin Invest 2005;115:1806–1815.

32. Tang N, Wang L, Esko J, Giordano FJ, Huang Y, Gerber HP, et al. Loss of HIF-1α in endothelial cells disrupts a hypoxia-driven VEGF autocrine loop necessary for tumorigenesis. Cancer Cell 2004;6: 485–495.

33. Weidemann A, Kerdiles YM, Knaup KX, Rafie CA, Boutin AT, Stockmann C, et al. The glial cell response is an essential component of hypoxia-induced erythropoiesis in mice. J Clin Invest 2009;119: 3373–3383.

34. Weidemann A, Krohne TU, Aguilar E, Kurihara T, Takeda N, Dorrell MI, et al. Astrocyte hypoxic response is essential for pathological but not developmental angiogenesis of the retina. Glia 2010;58: 1177–1185.

35. Halberg N, Khan T, Trujillo ME, Wernstedt-Asterholm I, Attie AD, Sherwani S, et al. Hypoxia-inducible factor 1α induces fibrosis and insulin resistance in white adipose tissue. Mol Cell Biol 2009;29: 4467–4483.

36. Kim JW, Tchernyshyov I, Semenza GL, Dang CV. HIF-1–mediated expression of pyruvate dehydrogenase kinase: a metabolic switch required for cellular adaptation to hypoxia. Cell Metab 2006;3: 177–185.

37. Papandreou I, Cairns RA, Fontana L, Lim AL, Denko NC. HIF-1 mediates adaptation to hypoxia by actively downregulating mitochondrial oxygen consumption. Cell Metab 2006;3:187–197.

38. Denko NC. Hypoxia, HIF1 and glucose metabolism in the solid tumour. Nat Rev Cancer 2008;8:705–713.

39. DeBerardinis RJ, Lum JJ, Hatzivassiliou G, Thompson CB. The biology of cancer: metabolic reprogramming fuels cell growth and proliferation. Cell Metab 2008;7:11–20.

40. Gerriets VA, Kishton RJ, Nichols AG, Macintyre AN, Inoue M, Ilkayeva O, et al. Metabolic programming and PDHK1 control CD4$^+$ T cell subsets and inflammation. J Clin Invest 2015;125:194–207.

41. Prigione A, Rohwer N, Hoffmann S, Mlody B, Drews K, Bukowiecki R, et al. HIF1α modulates cell fate reprogramming through early glycolytic shift and upregulation of PDK1-3 and PKM2. Stem Cells 2014;32:364–376.

42. Takubo K, Nagamatsu G, Kobayashi CI, Nakamura-Ishizu A, Kobayashi H, Ikeda E, et al. Regulation of glycolysis by Pdk functions as a metabolic checkpoint for cell cycle quiescence in hematopoietic stem cells. Cell Stem Cell 2013;12:49–61.

43. Tan Z, Xie N, Cui H, Moellering DR, Abraham E, Thannickal VJ, et al. Pyruvate dehydrogenase kinase 1 participates in macrophage polarization via regulating glucose metabolism. J Immunol 2015;194: 6082–6089.

44. Xie N, Tan Z, Banerjee S, Cui H, Ge J, Liu RM, et al. Glycolytic reprogramming in myofibroblast differentiation and lung fibrosis. Am J Respir Crit Care Med 2015;192:1462–1474.

45. Kottmann RM, Kulkarni AA, Smolnycki KA, Lyda E, Dahanayake T, Salibi R, Honnons S, Jones C, Isern NG, Hu JZ, et al. Lactic acid is elevated in idiopathic pulmonary fibrosis and induces myofibroblast differentiation via pH-dependent activation of transforming growth factor-β. Am J Respir Crit Care Med 2012;186: 740–751.

46. Tuder RM, Lara AR, Thannickal VJ. Lactate, a novel trigger of transforming growth factor-β activation in idiopathic pulmonary fibrosis. Am J Respir Crit Care Med 2012;186:701–703.

47. Stacpoole PW. Review of the pharmacologic and therapeutic effects of diisopropylammonium dichloroacetate (DIPA). J Clin Pharmacol J New Drugs 1969;9:282–291.

48. Stacpoole PW, Kurtz TL, Han Z, Langaee T. Role of dichloroacetate in the treatment of genetic mitochondrial diseases. Adv Drug Deliv Rev 2008;60:1478–1487.

49. Trimboli AJ, Cantemir-Stone CZ, Li F, Wallace JA, Merchant A, Creasap N, Thompson JC, Caserta E, Wang H, Chong JL, et al. Pten in stromal fibroblasts suppresses mammary epithelial tumours. Nature 2009;461: 1084–1091.

50. Trimboli AJ, Fukino K, de Bruin A, Wei G, Shen L, Tanner SM, Creasap N, Rosol TJ, Robinson ML, Eng C, et al. Direct evidence for epithelial–mesenchymal transitions in breast cancer. Cancer Res 2008; 68:937–945.

51. Kim JE, Nakashima K, de Crombrugghe B. Transgenic mice expressing a ligand-inducible cre recombinase in osteoblasts and odontoblasts: a new tool to examine physiology and disease of postnatal bone and tooth. Am J Pathol 2004;165: 1875–1882.

52. Akamatsu T, Arai Y, Kosugi I, Kawasaki H, Meguro S, Sakao M, Shibata K, Suda T, Chida K, Iwashita T. Direct isolation of myofibroblasts and fibroblasts from bleomycin-injured lungs reveals their functional similarities and differences. Fibrogenesis Tissue Repair 2013;6:15.

53. Giri SN, Hyde DM, Hollinger MA. Effect of antibody to transforming growth factor β on bleomycin induced accumulation of lung collagen in mice. Thorax 1993;48:959–966.

54. Ryan HE, Poloni M, McNulty W, Elson D, Gassmann M, Arbeit JM, Johnson RS. Hypoxia-inducible factor-1α is a positive factor in solid tumor growth. Cancer Res 2000;60:4010–4015.

55. Strutz F, Okada H, Lo CW, Danoff T, Carone RL, Tomaszewski JE, Neilson EG. Identification and characterization of a fibroblast marker: FSP1. J Cell Biol 1995;130:393–405.

56. Mitsuhashi A, Goto H, Saijo A, Trung VT, Aono Y, Ogino H, Kuramoto T, Tabata S, Uehara H, Izumi K, et al. Fibrocyte-like cells mediate acquired resistance to anti-angiogenic therapy with bevacizumab. Nat Commun 2015;6:8792.

57. Österreicher CH, Penz-Österreicher M, Grivennikov SI, Guma M, Koltsova EK, Datz C, Sasik R, Hardiman G, Karin M, Brenner DA. Fibroblast-specific protein 1 identifies an inflammatory subpopulation of macrophages in the liver. Proc Natl Acad Sci USA 2011;108:308–313.

58. Skalli O, Pelte MF, Peclet MC, Gabbiani G, Gugliotta P, Bussolati G, Ravazzola M, Orci L. α-smooth muscle actin, a differentiation marker of smooth muscle cells, is present in microfilamentous bundles of pericytes. J Histochem Cytochem 1989;37:315–321.

59. Verbeek MM, Otte-Höller I, Wesseling P, Ruiter DJ, de Waal RM. Induction of α-smooth muscle actin expression in cultured human brain pericytes by transforming growth factor-β 1. Am J Pathol 1994; 144:372–382.

60. Fries KM, Blieden T, Looney RJ, Sempowski GD, Silvera MR, Willis RA, Phipps RP. Evidence of fibroblast heterogeneity and the role of fibroblast subpopulations in fibrosis. Clin Immunol Immunopathol 1994;72:283–292.

61. Kotaru C, Schoonover KJ, Trudeau JB, Huynh ML, Zhou X, Hu H, Wenzel SE. Regional fibroblast heterogeneity in the lung: implications for remodeling. Am J Respir Crit Care Med 2006;173: 1208–1215.

62. Bernard K, Logsdon NJ, Ravi S, Xie N, Persons BP, Rangarajan S, Zmijewski JW, Mitra K, Liu G, Darley-Usmar VM, et al. Metabolic reprogramming is required for myofibroblast contractility and differentiation. J Biol Chem 2015;290: 25427–25438.

63. Kusko RL, Brothers JF II, Tedrow J, Pandit K, Huleihel L, Perdomo C, Liu G, Juan-Guardela B, Kass D, Zhang S, et al. Integrated genomics reveals convergent transcriptomic networks underlying chronic obstructive pulmonary disease and idiopathic pulmonary fibrosis. Am J Respir Crit Care Med 2016; 194:948–960.

64. Bauer Y, Tedrow J, de Bernard S, Birker-Robaczewska M, Gibson KF, Guardela BJ, Hess P, Klenk A, Lindell KO, Poirey S, et al. A novel genomic signature with translational significance for human idiopathic pulmonary fibrosis. Am J Respir Cell Mol Biol 2015;52: 217–231.

65. Kim S, Herazo-Maya JD, Kang DD, Juan-Guardela BM, Tedrow J, Martinez FJ, Sciurba FC, Tseng GC, Kaminski N. Integrative phenotyping framework (iPF): integrative clustering of multiple omics

data identifies novel lung disease subphenotypes. *BMC Genomics* 2015;16:924.

66. Bonnet S, Archer SL, Allalunis-Turner J, Haromy A, Beaulieu C, Thompson R, Lee CT, Lopaschuk GD, Puttagunta L, Bonnet S, *et al*. A mitochondria-K$^+$ channel axis is suppressed in cancer and its normalization promotes apoptosis and inhibits cancer growth. *Cancer Cell* 2007;11:37–51.

67. Abdelmalak M, Lew A, Ramezani R, Shroads AL, Coats BS, Langaee T, Shankar MN, Neiberger RE, Subramony SH, Stacpoole PW. Long-term safety of dichloroacetate in congenital lactic acidosis. *Mol Genet Metab* 2013;109:139–143.

68. Haase VH. Hypoxia-inducible factor signaling in the development of kidney fibrosis. *Fibrogenesis Tissue Repair* 2012;5:S16.

69. Mesarwi OA, Shin MK, Bevans-Fonti S, Schlesinger C, Shaw J, Polotsky VY. Hepatocyte hypoxia inducible factor-1 mediates the development of liver fibrosis in a mouse model of nonalcoholic fatty liver disease. *PLoS One* 2016;11:e0168572.

70. Palazon A, Goldrath AW, Nizet V, Johnson RS. HIF transcription factors, inflammation, and immunity. *Immunity* 2014;41:518–528.

71. Imtiyaz HZ, Simon MC. Hypoxia-inducible factors as essential regulators of inflammation. *Curr Top Microbiol Immunol* 2010;345: 105–120.

72. McMahon S, Charbonneau M, Grandmont S, Richard DE, Dubois CM. Transforming growth factor β1 induces hypoxia-inducible factor-1 stabilization through selective inhibition of PHD2 expression. *J Biol Chem* 2006;281:24171–24181.

73. Whitehouse S, Cooper RH, Randle PJ. Mechanism of activation of pyruvate dehydrogenase by dichloroacetate and other halogenated carboxylic acids. *Biochem J* 1974;141:761–774.

74. Michelakis ED, Webster L, Mackey JR. Dichloroacetate (DCA) as a potential metabolic-targeting therapy for cancer. *Br J Cancer* 2008; 99:989–994.

75. Gogvadze V, Orrenius S, Zhivotovsky B. Mitochondria as targets for cancer chemotherapy. *Semin Cancer Biol* 2009;19:57–66.

76. Michelakis ED, Sutendra G, Dromparis P, Webster L, Haromy A, Niven E, Maguire C, Gammer TL, Mackey JR, Fulton D, *et al*. Metabolic modulation of glioblastoma with dichloroacetate. *Sci Transl Med* 2010; 2:31ra34.

77. Deuse T, Hua X, Wang D, Maegdefessel L, Heeren J, Scheja L, Bolaños JP, Rakovic A, Spin JM, Stubbendorff M, *et al*. Dichloroacetate prevents restenosis in preclinical animal models of vessel injury. *Nature* 2014; 509:641–644.

78. Le Page LM, Rider OJ, Lewis AJ, Ball V, Clarke K, Johansson E, Carr CA, Heather LC, Tyler DJ. Increasing pyruvate dehydrogenase flux as a treatment for diabetic cardiomyopathy: a combined 13C hyperpolarized magnetic resonance and echocardiography study. *Diabetes* 2015;64:2735–2743.

79. McMurtry MS, Bonnet S, Wu X, Dyck JR, Haromy A, Hashimoto K, Michelakis ED. Dichloroacetate prevents and reverses pulmonary hypertension by inducing pulmonary artery smooth muscle cell apoptosis. *Circ Res* 2004;95:830–840.

80. Michelakis ED, McMurtry MS, Wu XC, Dyck JR, Moudgil R, Hopkins TA, Lopaschuk GD, Puttagunta L, Waite R, Archer SL. Dichloroacetate, a metabolic modulator, prevents and reverses chronic hypoxic pulmonary hypertension in rats: role of increased expression and activity of voltage-gated potassium channels. *Circulation* 2002;105: 244–250.

81. Semba H, Takeda N, Isagawa T, Sugiura Y, Honda K, Wake M, Miyazawa H, Yamaguchi Y, Miura M, Jenkins DM, *et al*. HIF-1α–PDK1 axis-induced active glycolysis plays an essential role in macrophage migratory capacity. *Nat Commun* 2016;7:11635.

82. Eckle T, Kewley EM, Brodsky KS, Tak E, Bonney S, Gobel M, Anderson D, Glover LE, Riegel AK, Colgan SP, *et al*. Identification of hypoxia-inducible factor HIF-1A as transcriptional regulator of the A2B adenosine receptor during acute lung injury. *J Immunol* 2014;192: 1249–1256.

83. Kinnaird A, Zhao S, Wellen KE, Michelakis ED. Metabolic control of epigenetics in cancer. *Nat Rev Cancer* 2016;16:694–707.

84. Cisneros J, Hagood J, Checa M, Ortiz-Quintero B, Negreros M, Herrera I, Ramos C, Pardo A, Selman M. Hypermethylation-mediated silencing of p14(ARF) in fibroblasts from idiopathic pulmonary fibrosis. *Am J Physiol Lung Cell Mol Physiol* 2012;303:L295–L303.

85. Neary R, Watson CJ, Baugh JA. Epigenetics and the overhealing wound: the role of DNA methylation in fibrosis. *Fibrogenesis Tissue Repair* 2015;8:18.

86. Robinson CM, Neary R, Levendale A, Watson CJ, Baugh JA. Hypoxia-induced DNA hypermethylation in human pulmonary fibroblasts is associated with Thy-1 promoter methylation and the development of a pro-fibrotic phenotype. *Respir Res* 2012;13:74.

87. Sanders YY, Ambalavanan N, Halloran B, Zhang X, Liu H, Crossman DK, Bray M, Zhang K, Thannickal VJ, Hagood JS. Altered DNA methylation profile in idiopathic pulmonary fibrosis. *Am J Respir Crit Care Med* 2012;186:525–535.

88. Allen E, Miéville P, Warren CM, Saghafinia S, Li L, Peng MW, Hanahan D. Metabolic symbiosis enables adaptive resistance to anti-angiogenic therapy that is dependent on mTOR signaling. *Cell Reports* 2016;15:1144–1160.

89. Fünfschilling U, Supplie LM, Mahad D, Boretius S, Saab AS, Edgar J, Brinkmann BG, Kassmann CM, Tzvetanova ID, Möbius W, *et al*. Glycolytic oligodendrocytes maintain myelin and long-term axonal integrity. *Nature* 2012;485:517–521.

90. Jiménez-Valerio G, Martínez-Lozano M, Bassani N, Vidal A, Ochoa-de-Olza M, Suárez C, García-Del-Muro X, Carles J, Viñals F, Graupera M, *et al*. Resistance to antiangiogenic therapies by metabolic symbiosis in renal cell carcinoma PDX models and patients. *Cell Reports* 2016;15:1134–1143.

91. Pisarsky L, Bill R, Fagiani E, Dimeloe S, Goosen RW, Hagmann J, Hess C, Christofori G. Targeting metabolic symbiosis to overcome resistance to anti-angiogenic therapy. *Cell Reports* 2016;15: 1161–1174.

92. Lyons RM, Keski-Oja J, Moses HL. Proteolytic activation of latent transforming growth factor-β from fibroblast-conditioned medium. *J Cell Biol* 1988;106:1659–1665.